Journal of Electrostatics 71 (2013) 611–617

Contents lists available at SciVerse ScienceDirect

Journal of Electrostatics

journal homepage: www.elsevier.com/locate/elstat

Review

Effect of humidity in charge formation and transport in LDPE

A. Aragoneses [a], I. Tamayo [c], A. Lebrato [a], J.C. Cañadas [a,*], J.A. Diego [a], D. Arencón [b], J. Belana [a]

[a] Dpt. de Física i Eng. Nuclear, Universitat Politècnica de Catalunya-Barcelona TECH., C/Colom 11, E-08222 Terrassa, Spain
[b] Centre Català del Plàstic-Dpt. Materials Science and Metallurgy, Universitat Politècnica de Catalunya-Barcelona TECH., C/Colom 114, E-08222 Terrassa, Spain
[c] Facultad de Ciencias de la Ingeniería, Universidad Tecnológica Equinoccial, Campus Santo domingo. Vía Chone Km 4.5., St Domingo de los Colorados, Ecuador

ARTICLE INFO

Article history:
Received 27 July 2012
Received in revised form
18 January 2013
Accepted 5 March 2013
Available online 17 March 2013

Keywords:
LDPE
Space charge
Charge-trapping
Electric discharge
Charge distribution
PEA
SPD
TSDC

ABSTRACT

Charge distribution and transport have been investigated in LDPE films with different humidity content under electric fields up to 130 MV/m. Pulsed electroacoustic measurements showed that, as water content increases, positive charge packets formation in the anode is enhanced and they propagate toward the cathode with higher transit speeds. Fits of surface potential decay measurements showed that charges in dry samples are injected directly into the volume, but the presence of moisture generates new trap centers in the surface of the material. This new trap level causes a charge accumulation on the surface, that gradually passes into the bulk. The observed behavior in development and propagation of charge packets are explained according to these results. Thermally stimulated depolarization current measurements showed a non-distributed relaxation associated to the new trap levels on the surface of the wet samples.

1. Introduction

Low Density Polyethylene (LDPE) is a non-polar polymer commonly used as insulating material due to its high electrical strength. With the increased interest in high voltage direct current applications (HVDC), these properties that make LDPE a good insulator may paradoxically generate some problems in the performance of the material. Its high trapping capacity along with the low carrier mobility can favor the formation of space charge in the material [1,2]. The presence of space charge in a dielectric material generates localized electric fields and plays an important role in aging processes [3]. Referring to the nature and depth of traps, it has been proposed that impurities and/or chain defects could be responsible for their existence in the material. Ieda [4] has performed a detailed study on PE inquiring into both theories.

Space charge in the material can be studied by the Pulsed Electroacoustic technique (PEA). In this technique a pulsed electric field is applied to the sample inducing the oscillation of space charges present through the material. The resulting pressure wave, related to the space charge distribution, is recorded as a function of time. More detailed explanation of this technique can be found in excellent treatises [5]. Although accepted space charge theories predict a continuous injection of charge with the generation of a space charge distribution until a steady state is reached [6], measurements at high and more recently medium electric fields showed that discrete injection of charge from the electrodes occurs [7,8]. Moreover, these injected 'packets' of charge retain the pulse-like nature as they transit through the insulation.

Several aspects of this phenomenon have been analyzed since then and a packet-like charge propagation has been observed in various conditions. Positive or negative packets are formed depending on the additives of the material and can be formed at the electrode or in the bulk. The phenomenon can be repeated in time or disappears after a certain number of pulses. The transit speed can be constant or slow down as the material is crossed, and the electric field necessary to originate these packets also varies from medium values (30–50 MV/m) to quite high fields (100–400 MV/m) ([9] and references herein). Models to explain the formation of charge packets at the electrode–polymer interface suggest that high electric fields, generated by the accumulation of charge at the

* Corresponding author. Tel.: +34 937398049; fax: +34 937398000.
E-mail address: juan.carlos.canadas@upc.edu (J.C. Cañadas).

0304-3886/$ – see front matter © 2013 Elsevier B.V. All rights reserved.
http://dx.doi.org/10.1016/j.elstat.2013.03.003

interface, can alter chain arrangement in the amorphous regions making tunneling injection possible [10]. The necessary hysteresis to obtain discrete charge injection can be obtained by this way. Nevertheless some controversy exists in the explanation of this phenomenon.

Another technique widely used to study charge transport in polymers is the Surface Potential Decay technique (SPD) [11–14]. In this technique, ions are deposited on a polymer film during a corona charging process. Because of their own electric field, electron or hole transfer to surface traps can take place generating a surface charge in the material. Depending on the potential applied during the corona charging process, carriers can be as well directly injected into the sample's bulk. In order to neutralize this charge, electrons or holes move by hopping to the opposite metalized surface. During this process, surface potential decay is related to charge transport in the material and can be analyzed applying some phenomenological models [13,15,16]. Some authors have studied SPD on LDPE [17] and recent works find accordance between experiments and this transport process interpretation [18–20].

Thermally stimulated depolarization current (TSDC) is a complementary technique suited as well to study charge relaxation processes in dielectrics [21–23]. In this technique an electret is formed by the application of an electric field to the sample that is then cooled down to freeze the polarization. The sample is then heated at a constant rate, thermally stimulating the depolarization of this charge. Fitting of the obtained discharge spectrum to some phenomenological models allow us to evaluate the activation energies of the observed relaxations as well as some other kinetic parameters. In a typical LDPE–TSDC spectrum a peak appears around −40 °C which corresponds to the α relaxation associated to the glass transition of the material. Free charge relaxation processes generate a peak around 50 °C followed by a complex electrical response when the material goes into the melt temperature range [24,25].

The effect of elevated humidity on electrical conductivity of different polymers can be found in the literature [26,27], however its influence in the packet-like charge formation is much less studied. In the present work we study the influence of humidity in LDPE charge transport mechanisms and we obtain some correlation between the formation of new trap levels associated to humidity and the generation of pulsed like charge transport. We analyze data obtained by PEA, SPD and TSDC and explain the increased ability to form packets of charge in the wet samples in the framework of existing theories in the subject.

2. Experimental

2.1. Sample preparation

A commercial grade of LDPE, Lupolen 1800H, was kindly supplied by Lyondel Basell. This is an extrusion grade LDPE having a melt flow rate of 19 g/min (ISO 1133: 2.16 kg, 190 °C). Films of 125 and 250 μm in thickness were obtained using a cast-film line, consisting of a single-screw extruder Collin Teach Line 20T-E ($L/D = 25$; $D = 20$ mm), a multi-manifold die and a calendaring rolls (Teach Line CR 72T). The die and calendering temperatures were 210 °C and 40 °C respectively. The prepared material was conditioned by a 1 h annealing at 75 °C to prevent possible morphological changes during later measurements in temperature.

Three types of samples, with different degrees of humidity, were prepared for the experiments. Among the samples kept at ambient conditions for several days in our laboratory (low humidity samples), some samples were kept at 30 °C in a humidity saturated ambient for 24 h (wet samples) and another set was kept in vacuum at 30 °C for 24 h (dry samples) previous to the experiments. In the case of samples for SPD and TSDC measurements, this humidification process was carried out after metallization of the sample.

2.2. DSC and FTIR measurements

Initial characterization of the samples was performed by differential scanning calorimetry (DSC) and Fourier Transform Infrared spectrometry (FTIR). DSC measurements were performed with a PerkinElmer Pyris 1 calorimeter, which was previously calibrated with standard samples of indium and lead. The samples (ca. 10 mg) were taken from the middle of the films. The melting and crystallization temperatures (T_m and T_c) were determined from the first heating and cooling scans, respectively. The crystalline fraction (X_m) was calculated by integration of the signal concerned, using the 100% crystalline LDPE crystallization enthalpy (288 g^{-1}) [28].

The IR pattern of LDPE was analyzed using a Nicolet 6700 spectrophotometer. The spectral resolution was 1 cm^{-1}, and the wavenumber interval analyzed was between 4000 and 400 cm^{-1}. For each measurement, 50 scans were performed. A Smart Orbit high-performance diamond single bounce attenuation total reflection (ATR) accessory was used. The depth of penetration of the equipment is 2.03 μm at 1000 cm^{-1}.

2.3. Pulsed electroacoustic measurements

PEA experimental set-up used in this work was a commercial PEA equipment 'Techimp PEA system'. A 'Spellman SL10' 130 kV high voltage power supply was used to polarize samples and data were recorded by means of a 'Tektronix TDS 5032' digital oscilloscope. Measurements were performed polarizing the samples up to 5 h at room temperature with applied voltages (V_p) between 2 and 20 kV. The pulse amplitude was 300 V and the pulse length was 40 ns. Charge distribution was measured continuously during polarization. Samples consisted in 8 cm square sheets and charge distribution measurements were performed in a 1 cm circular section at the middle of the sheet. The software used for deconvolution of the signal is a Labview based software provided by TechImp.

2.4. Surface potential decay measurements

Samples for surface potential measurements (SPD) were prepared coating a 1 cm diameter Al electrode on one side of the LDPE sheet by vacuum deposition. Measurements were carried out with a Trek model 347 electrostatic voltmeter. Samples were charged by the corona triode method [29]. The needle of the corona triode was kept at +10 kV during the charging process (3 s) while the grid was grounded and the rear side of the sample was kept at −1 kV. The distance between the sample and the grid was 8 mm. The gap between the grid and the needle was 25 mm. After the charging process, the sample was automatically moved to the measuring position, under the electrostatic voltmeter, in less than 0.5 s, and with the rear side of the sample grounded.

2.5. Thermally stimulated depolarization current

Samples for TSDC measurements were prepared by coating a 1 cm diameter Al electrode on one side of the LDPE sheet by vacuum deposition. In the measurements an air gap was present between the non-metallized side of the sample and the brass electrode. TSDC measurements were carried out in a non-commercial experimental setup, controlled by a Eurotherm-808 temperature programmer. The temperature, during measurements, was measured to an accuracy of 0.1 K by a PT100 sensor located close to the electrodes (in direct contact with the sample). A Keithley-6514 electrometer was employed for the current

measurements. All TSDC experiments were performed using the null window width polarization method (WP-TSDC) [30], except in the complete spectra discussed in Section 3.4. In the WP-TSDC method an electric field E_p was applied at a constant polarization temperature T_p for a polarization time t_p (isothermal polarization). Then the electric field was switched off and the sample was cooled down to a temperature T_d, where it remained for a time t_d previous to the depolarization process. With this isothermal polarization scheme the obtained depolarization peak can usually be described in a more simple way by a unique relaxation time as a good approach. Finally the sample was heated at a constant rate and the depolarization current was measured. Used values of these parameters in WP-TSDC measurements are: $E_p = 100$ MV/m, $t_p = 30$ min, $T_d = 8$ °C and $t_d = 30$ min. T_p varies in the different measurements between, $T_p = 15$ °C and $T_p = 50$ °C. The heating and cooling rate used for all TSDC measurements was 2 °C/min.

3. Results and discussion

3.1. Characterization of the humidity in the LDPE samples

Initial characterization of the samples was performed by differential scanning calorimetry (DSC) and Fourier Transform Infrared spectrometry (FTIR). DSC measurements in as prepared material shows no significant differences in the crystallinity degree regarding to the cooling roll temperature, so we selected 40 °C samples to perform the electrical tests. Once 'dry', 'low humidity' and 'wet' samples were prepared as described in the Experimental section, they were measured by FTIR to analyze the influence of the treatment. Fig. 1 shows the presence of a broad peak at ca. 3500 cm^{-1}, related with −OH groups, which ascertain for humidity in the surface of the wet samples.

Together with these results, mass measurements of the resulting samples were carried out to determine the % of water absorbed in each case. Results showed, as expected, very low water absorption with less than 0.4% weight increase in the wet sample with respect to the dry sample.

3.2. PEA measurements

Charge distribution and transport in low humidity samples were measured by PEA with applied fields between 12 MV/m and 120 MV/m. There is a threshold electric field around 80 MV/m above which charge transport takes place in the material following a packet like behavior. Positive charge packets flow from the anode and move toward the cathode with constant transit speeds of around 2.2×10^{-7} m/s. Fig. 2 shows this evolution for the first 845 s with an applied field of 100 MV/m. As has already been observed in other cases [31], this packet like charge transport is not stable and tends to disappear in long-term measurements. Another remarkable fact is the packet size remains almost constant in these samples as it propagates through the material.

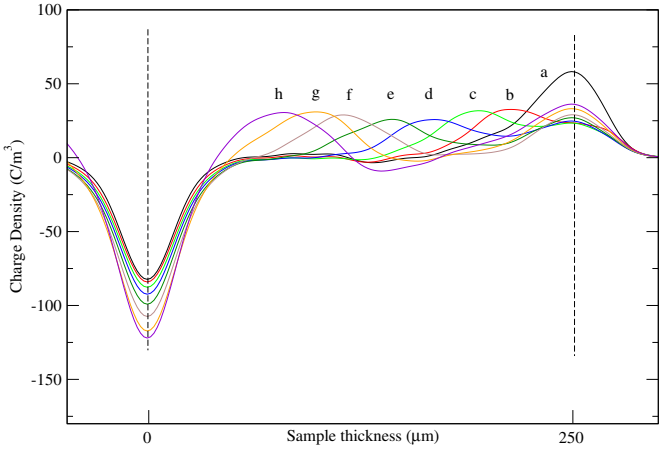

Fig. 2. PEA measurements in as received LDPE sample (low humidity) at 100 MV/m and different times after voltage application: (a) 145 s, (b) 245 s, (c) 345 s, (d) 445 s, (e) 545 s, (f) 645 s, (g) 745 s, (h) 845 s.

To analyze the effect of humidity in this phenomenon, wet samples were measured by PEA in the same conditions. Results obtained with these samples show several differences with the previous case. The threshold electric field for packet charge formation does not change appreciably, however packet propagation begins sooner in this case. This result indicates some increased tendency to form charge packets in the wet samples, also supported by the observed increase in the packet transit speed, of 4.1×10^{-7} m/s in this case (Fig. 3). Another remarkable fact is the progressive increase in the maximum of the charge density peak as the charge pulse propagates through the material.

Influence of humidity in charge distribution and transport was also evidenced performing PEA measurements with the dry

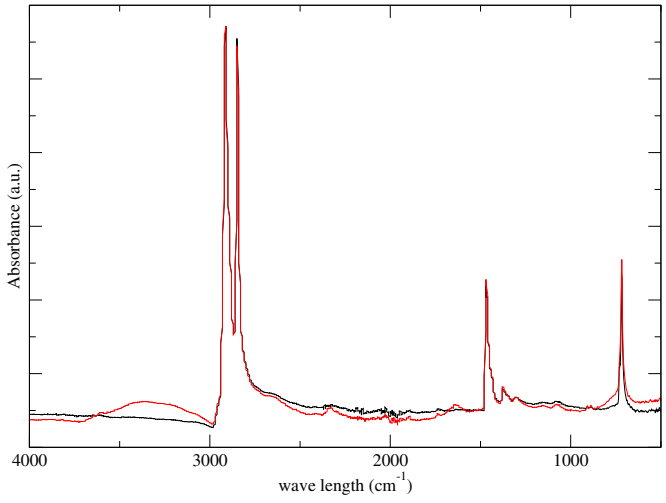

Fig. 1. Fourier transformed infrared spectroscopy of dry (black) and wet (red) LDPE samples. LDPE, space charge, charge-trapping. (For interpretation of the references to colour in this figure legend, the reader is referred to the web version of this article.)

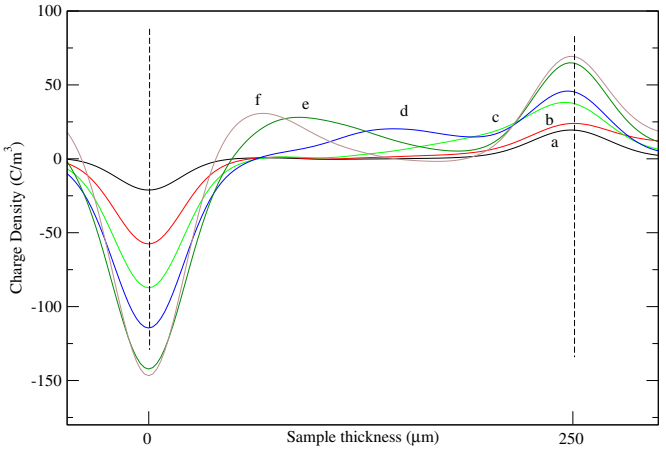

Fig. 3. PEA measurements in a LDPE wet sample at 100 MV/m and different times after voltage application: (a) 45 s, (b) 145 s, (c) 245 s, (d) 345 s, (e) 445 s, (f) 545 s.

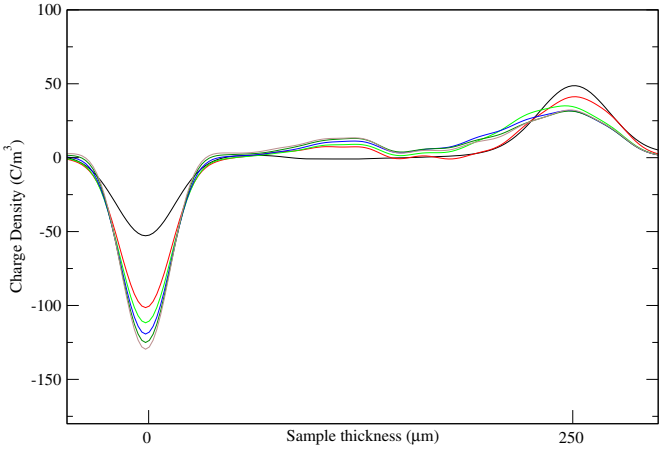

Fig. 4. First PEA measurements (up to 420 s) in a LDPE dry sample at 100 MV/m.

samples. In this case no packet like charge transport is developed at all with applied electric fields up to 130 MV/m (Fig. 4). Charge distribution profile in these samples evolves developing steady charge localized regions but with no packet like transport at all. All these results show that humidity in the sample is an important factor to take into account to understand, among other electrical properties, charge distribution and transport in LDPE.

3.3. Surface potential decay measurements

To study the effect of humidity in the electrical properties of LDPE we performed surface potential decay measurements (SPD) on samples with different levels of humidity. Fig. 5 shows the evolution in time of the normalized surface potential obtained with the three types of samples. A clear different behavior can be observed between the dry sample and those that present moisture to some extent. The presence of water in the material favors the surface voltage decay during the first seconds of the measurement. This behavior is related to an increase in surface trap density as well as structural disorder due to the presence of water as will be discussed below.

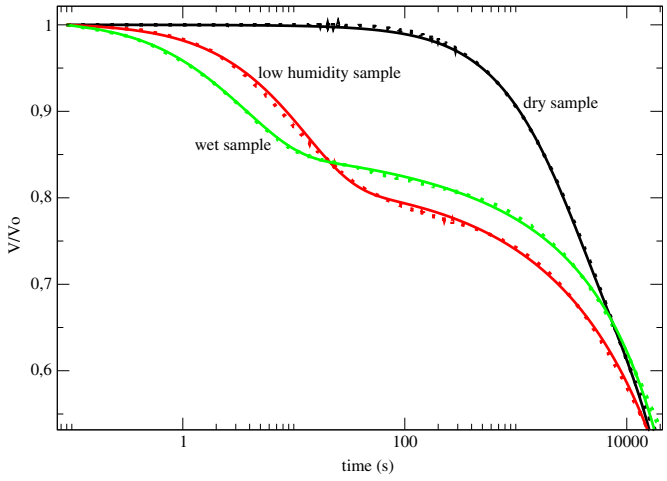

Fig. 5. Normalized plot for surface potential decay of wet (green), low humidity (red) and dry (black) samples. Doted lines correspond to experimental data while solid lines are the fits after equation (2). All samples were initially charged at 1 kV. (For interpretation of the references to colour in this figure legend, the reader is referred to the web version of this article.)

Table 1
Parameters obtained from the mathematical fit of SPD curves to equation (2).

	Dry	Low humidity	Wet
V_0 (V)	1040	1130	1050
μ_0 ($\times 10^{-15}$) ($m^2\ V^{-1}\ s^{-1}$)	3	400	900
r_r (s^{-1})	4×10^{-5}	10^{-5}	6×10^{-5}
r_t (s^{-1})	3×10^{-5}	0.08	0.24
a_1	0	0.65	0.92
α (s^{-1})	0	0.04	0.12
λ ($s^{-\beta}$)	0	0.005	0.01
β	0	0.4	0.3

3.3.1. Modeling of SPD results

Several authors have proposed different models to explain how charge transport takes place during a SPD measurement [13,15,16]. These models consider that, depending on the potential applied to the needle, in the corona charging, charge carriers are placed on the sample's surface, from where they jump to the bulk with a frequency α, or they can be directly injected into the samples bulk ($\alpha = \infty$).

After Toomer and Lewis model [15], once the charges are in the bulk, the band structure of the sample provides traps for the charge carriers, which drift through the sample hopping from one localized state to another, with a probability per unit time of a charge to release from the trap, r_r, and a probability per unit time to be retrapped in a different trapping center, r_t. This behavior takes into account the distribution of distances between localized sites available for carriers to hop as well as the dispersion of the potential barriers between these sites. This distribution in distances and/or energies affects the time a charge needs to hop from one site to another. This model assumes different number of adjustable parameters, depending on the type of traps and on the type of injection of the carriers (instantaneous or partially instantaneous), which at the end will depend on the characteristics of the sample. With the assumptions of the model, the superficial potential decay will follow the equation [15]:

$$V(t) - V_0 = \frac{-\mu_0}{2R}\left(\frac{V_0}{d}\right)^2 \int_0^t \left(r_r + r_t e^{-Rt}\right)\left[1 - \left(\sum_{n=1}^{\infty} a_n e^{-\alpha_n t}\right)^2\right] dt \quad (1)$$

In our study we consider the particular case, also considered in Ref. [15], with one type of traps in the sample's bulk and two types of injection processes: a fraction a_1 of the charges are initially placed on surface traps, from where they jump to the bulk at a certain rate α, while the rest, $(1 - a_1)$, are injected into the bulk immediately after the discharge ($\alpha_2 = \infty$). For highly disordered structures of some samples a dispersive term has to be also considered in order to explain the first decay of the surface potential (see Ref. [32]). In our case, we consider that humidity provides the sample's surface this disordered structure. After this, the surface potential of the charged sample decays as:

$$\frac{V(t)}{V_0} = 1 - \frac{V_0\mu_0}{2d^2R}\left(r_r t + \frac{r_t}{R}\left(1 - e^{-Rt}\right) + \frac{r_r a_1^2}{2\alpha}\left(1 - e^{-2\alpha t}\right)\right) - \frac{V_0\mu_0}{2d^2R}\left(\frac{r_t a_1^2}{R + 2\alpha}\left(1 - e^{-(R+2\alpha)t}\right)\right) - \lambda t^{\beta}, \quad (2)$$

where the last term (λt^{β}) is the dispersive term, $R = r_r + r_t$, d is the sample's width and μ_0 is the proper mobility of the sample. This is

the carrier's mobility between one trap and the next. We must distinguish this parameter from the effective mobility, that is influenced by the number of available traps and decays as the injected charges are being trapped and they remain trapped for certain amount of time [15].

The values of the free parameters, resulting from fitting equation (2) to the experimental data of Fig. 5, are shown in Table 1. The parameters were obtained by the downhill simplex method [33], where the seeds were chosen after the bibliography.

Five different SPD measurements were performed on each type of sample, while no significant differences were found in the fitted parameters. All the values obtained are in good agreement with those in Refs. [15,32].

We can see how the decay of the dry sample can be explained considering that all the charges are instantaneously injected into the sample's bulk. For the samples with humidity a new dynamics had to be considered in order to properly describe the decays. In this case some of the charges seem to be initially retained on the sample's surface and remain there a certain time before jumping into the bulk. Once inside the sample, the proper mobility is higher in this case than in the case of the dry sample. This parameter should be, in principle, similar in all the cases although it may also be influenced by the concentration of charges in the sample. At high carrier density, a decrease in the proper mobility is expected due to possible interactions between them. As charges do not penetrate instantaneously into the samples with humidity, the carrier density will be smaller and this difference could explain the increase in proper mobility.

A dispersive term has also to be considered in order to explain the effect of humidity on the samples. The higher the humidity the higher the disorder and the higher the fraction of charges initially placed on the surface. The probability for a charge to be trapped (r_t) rises with humidity, while the probability of a charge to release from a trap (r_r) remains constant, for the experimental parameters studied. We interpret this as due to a smaller initial concentration of charges in the bulk of the wet samples. This provides a higher number of available traps which facilitates charges to be trapped.

3.4. TSDC measurements

TSDC measurements have been performed to provide complementary information about conduction mechanisms in the material. This technique is able to discern between different trap levels, and thus different types of traps, as the depolarization of charges is thermally activated at different temperatures. Fig. 6 shows the complete spectrum obtained with the wet sample polarized at 30 °C for 30 min and cooled down to 8 °C with the electric field applied. In this figure, two depolarization peaks can be noted. At approximately 25 °C a first heteropolar peak appears, which is not present in dry samples. At about 50 °C a broad homopolar peak can be seen. The homopolar sign of this peak indicates probably that it is related to the relaxation of charge injected in the material from the electrodes.

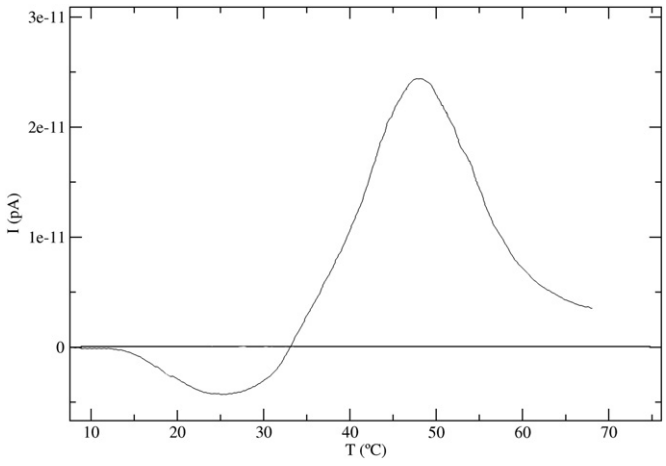

Fig. 6. Complete TSDC spectrum of a wet sample. Polarization parameters: $T_p = 30$ °C, $E_p = 100$ MV/m, $t_p = 30$ min and cooled down to $T_d = 8$ °C with the applied field on.

A second set of TSDC measurements was carried out, which consisted on successive charges and discharges of a wet sample in dry air ambient inside the oven where measurements were made. In each discharge the sample was heated up to 35 °C, fact that promotes the progressive drying of the sample. This drying process was checked as well by weight loss measurements of a sample subjected to the above mentioned cycles. This test sample showed a mass loss of almost 0.4%, slightly lower than that of the sample treated in vacuum (see Experimental section).

Fig. 7 shows the evolution of the heteropolar relaxation obtained in these measurements. A progressive decrease in the heteropolar response and a slight shift toward lower temperatures of the peak maximum is observed. After nine cycles the overall peak turns out to be scarcely observable. These results suggest that water molecules present in the sample during polarization are the main factor responsible of the heteropolar response.

To study the 50 °C broad homopolar peak another set of TSDC discharges were performed by the WP method with $E_p = 120$ MV/m and varying in this case the polarization temperature from $T_p = 15$ °C to $T_p = 50$ °C. Fig. 8 shows the spectra obtained in this case. As expected from the broad response observed in Fig. 6, there is a displacement of the peak with T_p which indicates a distributed relaxation. An optimal polarization temperature is obtained for $T_{po} = 30$ °C. At this polarization temperature is when the maximum discharge current, I_m, reaches a maximum value and from this temperature the thermal agitation begins to be dominant and the action of the electrical field diminishes.

3.4.1. Modelization of TSDC results

Free charge TSDC depolarization curves can be fitted to the general order kinetics model [34]. In this model a unique relaxation time is considered and the current intensity is assumed to follow the empirical equation:

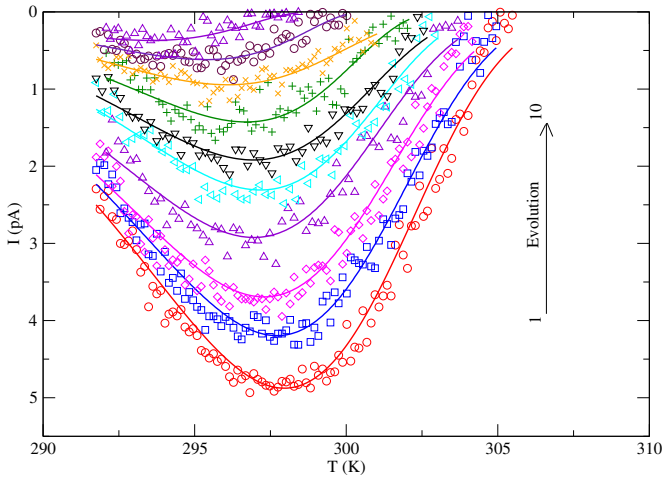

Fig. 7. WP-TSDC spectra of successive charge–discharge cycles of an initially wet sample in dry air (only plotted one of each two cycles). Continuous lines reproduce theoretical fit of the discharges. Polarization parameters: $E_p = 120$ MV/m, $T_p = 30$ °C $t_p = 30$ min, $T_d = 8$ °C and $t_d = 30$ min.

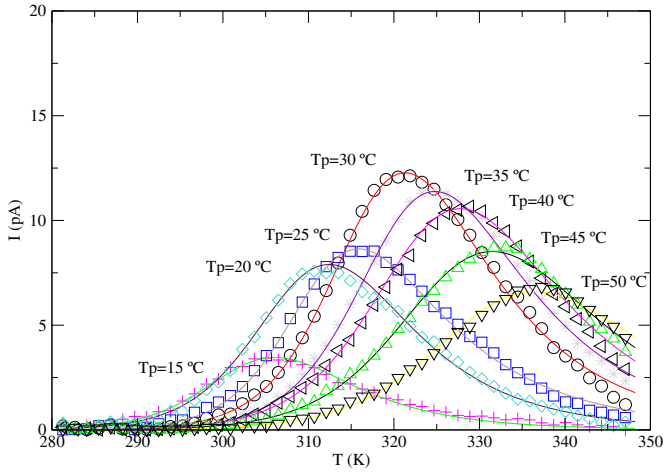

Fig. 8. WP-TSDC spectra of dry samples at different T_p. Continuous lines reproduce theoretical fit of the discharges. Polarization parameters: $E_p = 120$ MV/m, $t_p = 30$ min, $T_d = 8$ °C and $t_d = 30$ min. T_p varies in the different measurements between $T_p = 15$ °C and $T_p = 50$ °C.

$$I = -\frac{dn}{dt} = s_0' n^b \exp\left(-\frac{E_a}{kT}\right) \tag{3}$$

where n is the trapped charge at time t, E_a is the activation energy (the depth of the trapping sites in this model), T is the absolute temperature, k is the Boltzmann constant, s_0' is a preexponential factor and b is the kinetic order, an empirically determined parameter.

Integration of equation (3) simulating a TSDC discharge leads to the general kinetic order model equation:

$$I = n_0 s_0 \exp\left(-\frac{E_a}{kT}\right)\left[\frac{(b-1)s_0}{v}\int_{T_0}^{T}\exp\left(-\frac{E_a}{kT'}\right)dT' + 1\right]^{\frac{-b}{b-1}} \tag{4}$$

Where v is the heating rate, constant in our case, n_0 is the initial trapped charge and $s_0 = s_0' n_0^{(b-1)}$ is the preexponential frequency factor.

The b parameter is related to the interplay between the recombination and simultaneous retrapping rates. Equation (4) in the limit b tending to 1 (first order kinetics) reduces to the Randall and Wilkins equation that corresponds to the slow retrapping case, being recombination the dominant process [35]. In the case of $b = 2$, this equation reduces to the Garlick and Gibson equation [36] (second order kinetics is a case of strong retrapping probability). In the fit of experimental data, the values obtained habitually are around 1 and 2, or even higher ones in some cases that are difficult to interpret physically [37]. TSDC data were fitted to the general order kinetic equation by multidimensional minimization by the downhill simplex method [33].

In the calculations, n_0 was estimated from the total area of the TSDC peak and E_a, s_0 and b, are obtained fitting equation (4) to the data shown in Fig. 7. Table 2 summarizes the obtained values.

Table 2
Kinetic parameters obtained by fitting TSDC curves shown in Fig. 7 to the general kinetic-order model as a function of the cyclical charge–discharge.

Curve	1	2	3	4	5	6	7
n_0 (pC)	1400	1180	1010	746	581	477	310
E_a (eV)	1.70	1.73	1.73	1.76	1.80	1.82	1.84
S_0 (s^{-1})	4×10^{26}	1×10^{27}	1×10^{27}	7×10^{27}	3×10^{28}	7×10^{28}	2×10^{29}
b	0.974	0.986	0.989	0.890	0.890	0.913	0.817

Table 3
Kinetic parameters obtained by fitting TSDC curves shown in Fig. 8 to the general kinetic-order model as a function of the different temperatures of polarization.

T_p(°C)	15	20	25	30	35	40
n_0 (nC)	8.14	8.36	8.61	9.60	9.38	6.86
E_a (eV)	1.11	1.39	1.47	1.66	1.70	1.78
S_0 (s^{-1})	1×10^{14}	6×10^{18}	2×10^{20}	4×10^{23}	3×10^{24}	2×10^{26}
b	2.82	2.82	2.82	3.03	2.88	3.34

It can be noted that the initial trapped charge, n_0, decreases with successive cycles, i.e., with the progressive drying of the sample. This result suggests that the peak is related to the presence of water molecules in the LDPE sample.

A good overall adjustment is obtained to experimental data as shown by the continuous lines plotted in this figure. The estimated errors in E_a and b are about 1% and 5% respectively. In the case of the s_0 parameter, the obtained values are less reliable with estimated errors above 10%.

Values obtained for the b parameter shown in Table 2 are close to 1 in all the cases with a slight tendency to decrease. This indicates slow retrapping case and recombination as the main depolarization process, in good agreement with the stated hypothesis. The activation energy E_a does not change significantly throughout experiments, with a slight tendency to grow. Values obtained for the frequency factor, s_0, increase as the sample gets dried.

The parameters that fit the spectra of the second homopolar peak (Fig. 8) to equation (4) can be seen in Table 3. This homopolar peak corresponds, as stated above, to charge injected from the electrodes during the polarization process, and thus it is related to the traps through which the charge packets can move. Obtained results show a high distribution of trap energy levels comprised in the range $E_a = 1.11$ eV for $T_p = 15$ °C to more than 1.8 eV as T_p increases. We must notice that the decrease in E_a observed for $T_p = 45$ °C and $T_p = 50$ °C is an experimental artifact, as recorded curves are not completed in these cases because we stopped the scan before the peak ended, to avoid sample degradation.

The highest trapped charge, n_0, corresponds to $T_P = 30$ °C which is the optimum polarization temperature for this relaxation. With regard to the b parameter, it shows approximately a constant value close to 3. This fact indicates that recombination has dropped in favor of retrapping as the main charge release process. Prakash et al. proposed for this case around 33% of recombination processes in front of 67% of retrapping [37]. In any case, the predominance of retrapping supports the assumption that injected charge travel through the material and is released at different traps from where it was generated.

4. Conclusions

Charge pulse generation and propagation in LDPE measured by PEA show clear differences in dry, low humidity and wet samples, only attributable to the presence of water in the material. As water content increases, positive charge packets formation in the anode is enhanced and they propagate toward the cathode with higher transit speeds. Weight measurements, however, show that low absorption of water takes place (around 0.4%) even in the samples kept at 30 °C in a humidity saturated ambient for 24 h. This fact is due to the very low polarity of PE main polymer chain and water absorption, presumably, takes place close to the surface of the material.

SPD measurements also show significant differences between wet and dry samples. Moisture in the LDPE brings up a new process in the injection of charge carriers. While charges in dry samples are injected directly into the volume, our results indicate that moisture causes a charge accumulation on the surface, that gradually passes into the bulk. This charge accumulation associated with the

moisture has also been found in the TSDC and PEA measurements. This suggests that water molecules are placed on the surface, creating a new type of traps that affect the rate at which charges penetrate the sample. This behavior may promote the development of charge pulses propagating through the sample. Once charges begin to cross the sample, the charge density inside is lower, with more available traps. The fits, which indicate that the probability of falling into a trap increases with moisture, while the probability of release does not change, supports this idea. In turn, the proper mobility of charge carriers rises with moisture, perhaps related to a lower presence of other carriers that shield their movement.

TSDC measurements in wet samples show a non-distributed relaxation peak around 298 K. The gradual disappearance of this peak with successive cyclical discharges, and its absence in dry samples, indicates that it is originated by the presence of moisture in the sample. This trap level may be the one responsible of the charge accumulation on the surface of the material detected in SPD results modelization. A second distributed peak appears in TSDC measurements in all the samples (dry and wet) between 307 K and 337 K. This relaxation is characteristic of LDPE and is associated to trapping centers in the bulk of the material.

Acknowledgments

This work has been financed by the Agència de Gestió d'Ajuts Universitaris i de Recerca de la Generalitat de Catalunya (2009SGR1168).

References

[1] A. Cavallini, D. Fabiani, G. Mazzanti, G.C. Montanari, L. Simoni, Life estimation of dc insulation systems in the presence of voltage-polarity inversions, in: Conference Records of the 2000 IEEE ISEI (August 2000), pp. 114–122. Anaheim, USA.
[2] A. Cavallini, D. Fabiani, G. Mazzanti, G.C. Montanari, Life model based on space-charge quantities for hvdc polymeric cables subjected to voltage-polarity inversions, IEEE Trans. Diel. Electr. Insul. 9 (4) (2002) 514–523.
[3] L.A. Dissado, J.C. Fothergill, Electrical Degradation and Breakdown in Polymers, Peter Peregrinus LTD, London, 1992.
[4] M. Ieda, Electrical conduction and carrier traps in polymeric materials, IEEE Trans. Electr. Insul. EI-19 (1983) 162–167.
[5] T. Takada, Acoustic and optical methods for measuring electric charge distributions in dielectrics, IEEE Trans. Diel. Electr. Insul. 6 (5) (1999) 519–547.
[6] A. Many, G. Rakavy, Theory of transient space charge limited current in solids in the presence of trapping, Phys. Rev. 126 (6) (1993) 1980–1988.
[7] H.K. Xie, K.C. Kao, A study of the low density regions developed in liquified polyethylene under high electric fields, IEEE Trans. Electr. Insul. 20 (1985) 293–297.
[8] N. Hozumi, H. Suzuki, T. Okamoto, Direct observation of time-dependent space charges profiles in xlpe cable under high electric fields, IEEE Trans. Diel. Electr. Insul. 1 (6) (1994) 1068–1076.
[9] L.A. Dissado, The origin and nature of 'charge packets': a short review, in: 10th IEEE International Conference on Solids Dielectrics (ICSD) (4–9 July 2010), pp. 1–6. Postdam, Germany.
[10] T.J. Lewis, J.P. Llewellyn, M.J. van der Sluijs, Electrokinetic properties of metal-dielectric interfaces, IEE Proc. A. Sci., Meas. Technol. 140 (5) (1993) 385–392.
[11] G. Chen, H. Xiao, C. Zhu, Charge dynamic characteristics in corona-charged polytetrafluoroethylene film electrets, J. Zhejiang Univ. Sci. 8 (2004) 923–927.
[12] R. Coelho, L. Levy, D. Sarrail, On the natural decay of corona charged insulating sheets, Phys. Stat. Solidi A 94 (1986) 289–298.
[13] P. Llovera, P. Molinié, New methodology for surface potential decay measurements: application to study charge injection dynamics on polypropylene films, IEEE Trans. Diel. Electr. Insul. 11 (2004) 1049–1056.
[14] J. Zha, G. Chen, Z. Dang, Y. Yin, The influence of tio_2 nanoparticle incorporation on surface potential decay of corona-resistant polyimide nanocomposite films, J. Electrostat. 69 (2011) 255–260.
[15] R. Toomer, T.J. Lewis, Charge trapping in corona-charged polyethylene films, J. Phys. D: Appl. Phys. 13 (1980) 1343–1356.
[16] H. von Berlepsh, Interpretations of surface potential kinetics in hdpe by a trapping model, J. Phys. D: Appl. Phys. 21 (1985) 1155–1170.
[17] T. Mizutani, Y. Taniguchi, M. Ishioka, Charge decay and space charge in corona-charged ldpe, in: 11th International Symposium on Electrets, ISE 11 (10 December 2002), pp. 15–18. Melbourne, Australia.
[18] S. Ziari, Z. Sahli, A. Bellel, Mobility dependence on electric field in low density polyethylene (ldpe), M. J. Condens. Matter 12 (3) (2010) 223–226.
[19] G.M. Sessler, Charge distribution and transport in polymers, IEEE Trans. Diel. Electr. Insul. 24 (1997) 614–627.
[20] L. Zhang, Z. Xu, G. Chen, Decay of electric charge on corona charged polyethylene, J. Phys. Conf. Ser. 142 (2008) 1–4.
[21] J. Van Turnhout, Thermally Stimulated Discharge of Polymer Electrets, Elsevier, Amsterdam, 1980, pp. 83–96. (Chapter 3).
[22] C. Lavergne, C. Lacabanne, A review of thermo-stimulated current, IEEE Electr. Insul. Mag. 9 (1993) 5–21.
[23] G.M. Sessler, Electrets, third ed., vol. 2, Laplacian, Morgan Hill, CA, 1999, pp. 41–80. (Chapter 10).
[24] I. Tamayo, J. Belana, J.C. Cañadas, M. Mudarra, J.A. Diego, J. Sellarès, Thermally stimulated depolarization currents of crosslinked polyethylene relaxations in the fusion range of temperatures, J. Polym. Sci. Part. B: Polym. Phys. 41 (2003) 1412–1421.
[25] I. Tamayo, J. Belana, J.A. Diego, J.C. Cañadas, M. Mudarra, J. Sellarès, Space charge studies of crosslinked polyethylene midvoltage cable insulation by thermally stimulated depolarization current, infrared/fourier transform infrared, and scanning electron microscopy, J. Polym. Sci. Part. B: Polym. Phys. 42 (2004) 4164–4174.
[26] F. Belluci, I. Khamis, S.D. Senturia, R.M. Latanision, Moisture effects on the electrical conductivity of kapton polyimide, J. Electrochem. Soc. 137 (1990) 1778–1784.
[27] N.A. Galichin, M.E. Borisova, The influence of elevated humidity on the stability of the electret state in polyimide films, Russ. Electr. Engin. 78 (2007) 129–132.
[28] B. Wunderlich, Thermal Analysis, Academic Press, New York, USA, 1990.
[29] C.J. Dias, J.N. Marat-Mendes, J.A. Giacometti, Effects of a corona discharge on the charge stability of teflon fep negative electrets, J. Phys. D: Appl. Phys. 22 (1989) 663–669.
[30] M. Zielinski, M. Kryszewski, Thermal sampling technique for the thermally stimulated depolarization currents, Phys. Stat. Solidi A42 (1977) 305–314.
[31] K. Matsui, Y. Tanaka, T. Takada, Numerical analysis of packet-like charge behavior in low-density polyethylene under dc high electric field, IEEE Trans. Diel. Electr. Insul. 15 (3) (2008) 841–850.
[32] A. Aragoneses, M. Mudarra, J. Belana, J.A. Diego, Study of dispersive mobility in polyimide by surface voltage decay measurements, Polymer 49 (2008) 2440–2443.
[33] J.A. Nelder, R. Mead, A simplex method for function minimization, Comput. J. 7 (1965) 308–313.
[34] R. Chen, Y. Kirsh, Analysis of Thermally Stimulated Processes, Oxford:Pergamon Press, Oxford, 1981.
[35] J.T. Randall, M.H.F. Wilkins, Phosphorescence and electron traps i. the study of traps distributions, Proc. Roy. Soc. (London) A 184 (999) (1945) 365–389.
[36] G.F.J. Garlick, A.F. Gibson, The electron trap mechanism of luminescence in sulfide and silicate phosphors, Proc. Phys. Soc. 60 (1948) 574–583.
[37] J. Prakash, S.K. Rai, P.K. Singh, H.O. Gupta, Mechanisms inherent in the thermoluminescence processes, Indian J. Pure Appl. Phys. 42 (2004) 565–571.